Anal. Chem. **2006,** *78,* 3643−3650

Piezo Dispensed Microarray of Multivalent Chelating Thiols for Dissecting Complex Protein−Protein Interactions

Goran Klenkar,[†] Ramûnas Valiokas,[‡] Ingemar Lundström,[⊥] Ali Tinazli,[§] Robert Tampé,[§] Jacob Piehler,[§] and Bo Liedberg[†,*]

Division of Molecular and Applied Physics, Department of Physics, Chemistry, and Biology, Linköping University, S-581 83 Linköping, Sweden, Molecular Compounds Physics Laboratory, Institute of Physics, Savanoriu 231, LT-023 00 Vilnius, Lithuania, and Institute of Biochemistry, Johann Wolfgang Goethe-University, Max-von-Laue-Str. 9, D-60438 Frankfurt, Germany

The fabrication of a novel biochip, designed for dissection of multiprotein complex formation, is reported. An array of metal chelators has been produced by piezo dispensing of a bis-nitrilotriacetic acid (bis-NTA) thiol on evaporated gold thin films, prestructured with a microcontact printed grid of eicosanethiols. The bis-NTA thiol is mixed in various proportions with an inert, tri(ethylene glycol) hexadecane thiol, and the thickness and morphological homogeneity of the dispensed layers are characterized by imaging ellipsometry before and after back-filling with the same inert thiol and subsequent rinsing. It is found that the dispensed areas display a monotonic increase in thickness with increasing molar fraction of bis-NTA in the dispensing solution, and they are consistently a few Ångströms thicker than those prepared at the same molar fraction by solution self-assembly under equilibrium-like conditions. The bulkiness of the bis-NTA tail group and the short period of time available for chemisorption and in-plane organization of the dispensed thiols are most likely responsible for the observed difference in thickness. Moreover, the functional properties of this biochip are demonstrated by studying multiple protein−protein interactions using imaging surface plasmon resonance. The subunits of the type I interferon receptor are immobilized as a composition array determined by the surface concentration of bis-NTA in the array elements. Ligand dissociation kinetics depends on the receptor surface concentration, which is ascribed to the formation of a ternary complex by simultaneous interaction of the ligand with the two receptor subunits. Thus, multiplexed monitoring of binding phenomena at various compositions (receptor densities) offers a powerful tool to dissect protein−protein interactions.

Protein arrays and multifunctional biochips are powerful tools in the search for an improved understanding and novel applications of the proteome, the tremendous set of posttranslationally modified gene products that are responsible for vital processes in all living organisms.[1] Each protein is assumed to be involved in about five interactions (on average), and it often exerts its function in multiprotein complexes. The huge complexity of such architectures, for example, in cellular protein interaction networks, therefore, requires highly multiplexed and precisely tuned assays.[2] Unlike classical spectroscopic methods, spatially controlled deposition of proteins into an array format enables simultaneous mapping of multiple interactions,[3] in real time, using label-free detection methods.[4−6] A key prerequisite for such techniques is accurate immobilization of proteins onto solid supports in a native and functional manner.

Solution self-assembly of functional alkanethiols onto noble metal surfaces is a convenient way to control the surface composition, orientation, and presentation of biological macromolecules, such as proteins, peptides, and carbohydrates.[7,8] Moreover, such self-assembled monolayers (SAMs) have been used to obtain ultrahigh array element densities by employing soft lithography techniques, such as microcontact printing (μCP)[9] and nanopatterning, for example, with dip-pen nanolithography.[10,11] One attractive route to generate functional layers and micropat-

* Corresponding author. Phone: +46-13-281877. Fax: +46-13-288969. E-mail: bol@ifm.liu.se.

[†] Division of Molecular Physics, Department of Physics, Chemistry, and Biology, Linköping University.

[‡] Institute of Physics.

[§] Johann Wolfgang Goethe-University.

[⊥] Applied Physics, Department of Physics, Chemistry and Biology, Linköping University.

(1) Zhu, H.; Snyder, M. *Curr. Opin. Chem. Biol.* **2003**, *7*, 55−63.
(2) Piehler, J. *Curr. Opin. Struct. Biol.* **2005**, *15*, 4−14.
(3) Ramachandran, N.; Hainsworth, E.; Bhullar, B.; Eisenstein, S.; Rosen, B.; Lau, A. Y.; Walter, J. C.; Labaer, J. *Science* **2004**, *305*, 86−90.
(4) Cooper, M. A. *Anal. Bioanal. Chem.* **2003**, *377*, 834−842.
(5) Wegner, G. J.; Lee, H. J.; Corn, R. M. *Anal. Chem.* **2002**, *74*, 5161−5168.
(6) Wegner, G. J.; Lee, N. J.; Marriott, G.; Corn, R. M. *Anal. Chem.* **2003**, *75*, 4740−4746.
(7) Senaratne, W.; Andruzzi, L.; Ober, C. K. *Biomacromolecules* **2005**, *6*, 2427−2448.
(8) Ulman, A. *Chem. Rev.* **1996**, *96*, 1533−1554.
(9) Xia, Y. N.; Whitesides, G. M. *Angew. Chem., Int. Ed.* **1998**, *37*, 551−575.
(10) Ginger, D. S.; Zhang, H.; Mirkin, C. A. *Angew. Chem., Int. Ed.* **2004**, *43*, 30−45.
(11) Love, J. C.; Estroff, L. A.; Kriebel, J. K.; Nuzzo, R. G.; Whitesides, G. M. *Chem. Rev.* **2005**, *105*, 1103−1170.

10.1021/ac060024+ CCC: $33.50
Published on Web 04/21/2006

Chart 1. Alkylthiol Used for Array Fabrication

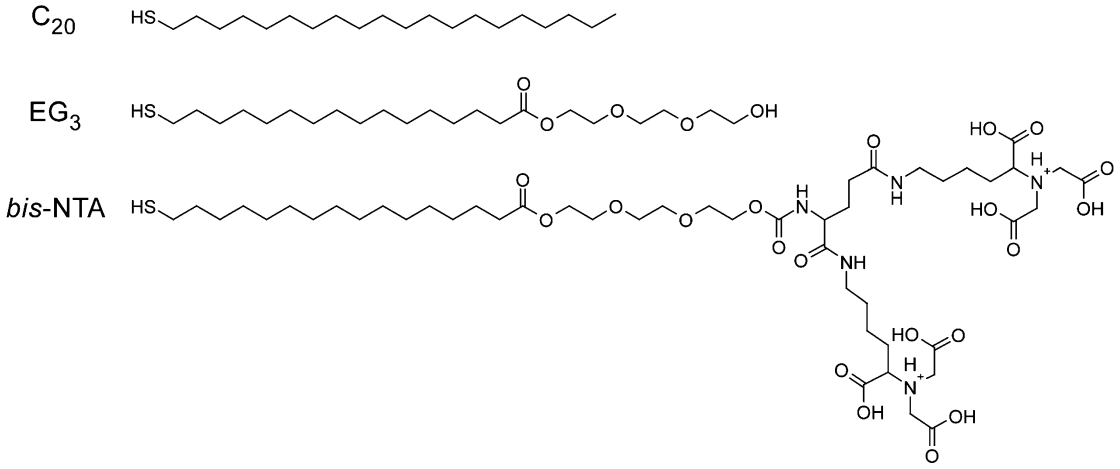

terns of oriented recombinant proteins fused to oligohistidine tags (His-tags) involves mixed SAMs prepared from solutions containing alkanethiols with terminal *N*-nitrilotriacetic acid (NTA) groups.[6,12−14] This concept has been borrowed from metal ion affinity chromatography, an often used method in protein purification.[15−17] Recently, it has been shown that the affinity of the His-tagged proteins can be further improved by employing multivalent chelator groups.[12] A chelator head containing two NTA moieties (bis-NTA) offers stable protein immobilization, even at low surface concentration, which has proven particularly useful for analysis of ligand−receptor interactions in real time.[18,19] In contrast to the traditional mono-NTA moiety, stoichiometric protein loading to immobilized bis-NTA is possible.[18] Hence, mixed bis-NTA SAMs provide a convenient platform for the fabrication of protein layers with precisely defined surface compositions. This feature is particularly important for dissecting cooperative interactions in multiprotein complexes, which are very difficult to assess in the case of low-affinity interactions.

This report focuses on the microfabrication and characterization of bis-NTA density arrays that are designed for studies of the interactions between immobilized receptor domains and the ligand. The arrays are prepared by piezo-dispensing bis-NTA thiol solutions onto gold surfaces, prestructured with a microcontact printed grid of hydrophobic molecules. Imaging null ellipsometry[20,21] is employed to study the morphology and thickness of the spotted domains, consisting of a mixture of thiols terminated with the inert (protein-repellent) tri(ethylene glycol) (EG_3) and bis-NTA groups. Further on, we discuss the properties of the bis-NTA arrays with controlled surface concentration and demonstrate the power of the generated arrays by analyzing in real time with imaging surface plasmon resonance (SPR)[22] the ligand-induced cross-linking of the extracellular domains of the type I interferon receptor.

EXPERIMENTAL SECTION

Substrates. The gold substrates for chip production were manufactured in a Balzers UMS 500 P system by electron-beam deposition. For ellipsometric samples, 2000 Å of gold was evaporated onto silicon(100) wafers, precoated with a 25-Å-thick titanium adhesion layer. For SPR-measurements 300 Å of gold was evaporated onto SF10 glass substrates (Schott, Germany), precoated with 10 Å of titanium. The base pressure was below 10^{-9} mbar, and the evaporation pressure was always below 10^{-7} mbar. The gold evaporation rate was 10 and 2 Å/s for the ellipsometric and SPR samples, respectively, and the rate for the titanium deposition was 1 Å/s for both samples. Before use, the gold chips were cleaned for 5 min at 85 °C in an SC1 solution containing a 5:1:1 mixture of MilliQ water, 30% hydrogen peroxide, and 25% ammonia, then rinsed in MilliQ water and dried in a stream of nitrogen.

Preparation of Chips. The thiols used for patterning bis-NTA density arrays are shown in Chart 1. Eicosanethiol (C_{20}) was a generous gift from Prof. Dave Allara (Penn State University, State College, PA). The synthesis of the bis-NTA thiol and the EG_3 thiol has been described previously, along with the procedure to characterize solution-incubated SAMs of their mixtures.[19] In our present work, however, ethanol was used as a solvent for the SAM formation.

Figure 1 outlines the main steps of the array fabrication procedure. The poly(dimethylsiloxane) (PDMS) stamp production was performed as described elsewhere.[23] The pattern consisted of 125-μm-wide protruding frames separating a 10 × 10 array of 375-μm-wide recessed squares. Prior to use, the stamp was thoroughly rinsed in ethanol and dried in a stream of nitrogen. The stamp was inked with 0.2 mM C_{20} in ethanol for 30−60 s. After the stamp had been carefully dried in a stream of nitrogen,

(12) Lata, S.; Reichel, A.; Brock, R.; Tampé, R.; Piehler, J. *J. Am. Chem. Soc.* **2005**, *127*, 10205−10215.
(13) Liley, M.; Keller, T. A.; Duschl, C.; Vogel, H. *Langmuir* **1997**, *13*, 4190−4192.
(14) Sigal, G. B.; Bamdad, C.; Barberis, A.; Strominger, J.; Whitesides, G. M. *Anal. Chem.* **1996**, *68*, 490−497.
(15) Hochuli, E.; Dobeli, H.; Schacher, A. *J. Chromatogr.* **1987**, *411*, 177−184.
(16) Porath, J.; Carlsson, J.; Olsson, I.; Belfrage, G. *Nature* **1975**, *258*, 598−599.
(17) Ueda, E. K.; Gout, P. W.; Morganti, L. *J. Chromatogr., A* **2003**, *988*, 1−23.
(18) Lata, S.; Piehler, J. *Anal. Chem.* **2005**, *77*, 1096−1105.
(19) Tinazli, A.; Tang, J.; Valiokas, R.; Picuric, S.; Lata, S.; Piehler, J.; Liedberg, B.; Tampe, R. *Chem.—Eur. J.* **2005**, *11*, 5249−5259.
(20) Jin, G.; Tengvall, P.; Lundstrom, I.; Arwin, H. *Anal. Biochem.* **1995**, *232*, 69−72.
(21) Liu, A. H.; Wayner, P. C.; Plawsky, J. L. *Appl. Opt.* **1994**, *33*, 1223−1229.
(22) Johansen, K.; Arwin, H.; Lundstrom, I.; Liedberg, B. *Rev. Sci. Instrum.* **2000**, *71*, 3530−3538.
(23) Zhou, Y.; Valiokas, R.; Liedberg, B. *Langmuir* **2004**, *20*, 6206−6215.

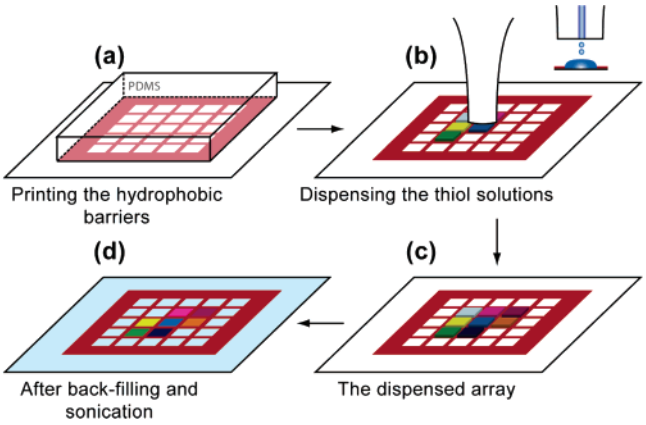

Figure 1. Schematic illustration of the various steps used to fabricate the array of thiols on the gold biochip: (a) printing the hydrophobic C_{20} barriers with the PDMS stamp; (b) dispensing different molar ratios of bis-NTA in spots defined by the hydrophobic barriers (inset shows a close-up of the nozzle and the dispensed liquid inside the hydrophobic barriers); (c) the dispensed array where different colors represent different molar ratios of bis-NTA; and (d) the ready-to-use biochip after back-filling with EG_3 and sonication in ethanol to remove weakly adsorbed multilayers and contaminants.

it was put on the gold surface for 1 min to generate hydrophobic, 125-μm-wide, C_{20} SAM barriers. Mixtures of bis-NTA and EG_3 were prepared in ethanol and loaded into a 60-μm-diameter, piezo-driven, glass capillary (Microdrop, Germany) facing the sample surface. The sample was mounted on a manual x/y stage. Since the printing was done by hand without repeatable alignment, the position of the array elements had to be revealed. This was done by cooling the surface slightly below the dew point with a Peltier element, thus allowing water to condense on the chip surface before deposition of the bis-NTA thiol solution. The high relative differences in surface energy between the printed hydrophobic barriers and the unmodified gold squares gave a contrast in water condensation, thereby making the pattern clearly visible through an optical microscope. The relative humidity of the ambient air was kept at 50−60%, giving a dew point of ~12 ± 1 °C. Once the dispenser head was correctly positioned above the square to be filled, the temperature was raised above the dew point to let the water evaporate. Successively and pairwise, a total of 14 drops (total volume of 1.6 nL for a capillary providing 60 μm droplets) were ejected from the dispenser at an interval of ~1−2 s. This facilitated a controlled delivery of material to the array element. The ethanol normally evaporated within 5−30 s, leaving a thin solid layer of thiols in the square. The dispenser head was cleaned twice in ethanol with the system's integrated cleaning function, involving sonication at 12 kHz, before loading the next thiol mixture aliquot to be dispensed. Possible contaminants from the surrounding air were kept to a minimum by keeping the whole dispensing unit in a protective box. Immediately after dispensing the bis-NTA thiol solutions, the sample was incubated in 1 mM EG_3 dissolved in ethanol for at least 2 h to back-fill the uncovered regions of the chip. After the incubation, the surface was thoroughly rinsed in ethanol and sonicated for 10 min in ethanol to remove physisorbed thiol multilayers.

Imaging Null-Ellipsometry and SPR. Ellipsometric measurements were performed on an EP^3 imaging null-ellipsometer (Nanofilm, Germany) equipped with a xenon lamp. Imaging SPR experiments were performed on the same instrument using an SPR cell. The combination of SPR with ellipsometry has been discussed earlier,[24] and its application to monitor biomolecular interactions has been reported;[25,26] however, in our (imaging) setup, it is also possible to resolve the surface laterally and to monitor different regions of the biochip in parallel. The SPR cell utilizes the Kretschmann setup for SPR-measurements[27] and consists of a holder for a 60° SF 10 prism and a flow cell. All measurements were performed at a wavelength of 532 nm, selected from the spectrum of the xenon lamp by an interference filter. The angles of incidence were 60° for ellipsometric and 63.5° for SPR measurements. The complex refractive index of the gold film was measured immediately after the SC1 wash with the imaging ellipsometer. A refractive index of 1.5[28] was assumed for the organic layers on the gold chips, and it was inserted, together with the refractive index of the gold substrate, into a three-layer optical model for calculation of the *effective* layer thickness. Residual linear gradients in the generated thickness maps were corrected interactively with software tools of the instrument. Tilted planes were added to the data under visual control until a flat background was achieved. The ellipsometric thicknesses were averaged over the regions of interest, excluding visible contaminants or fabrication defects. Indicated error levels represent the standard deviation in the respective region. For imaging SPR-measurements, the ellipsometric angles Ψ and Δ, averaged over each region of interest, were recorded over time at a sampling interval of 20 s. Sensorgrams are presented as the change of Ψ over time.

Binding Assays. Prior to binding assays, the chip was incubated for 10 min in a solution of 1 mg/mL bovine serum albumin (BSA) in 50 mM Hepes, pH 7.4, and 150 mM NaCl to block nonspecific binding to the hydrophobic (C_{20}) grid. Ligand binding assays were carried out with the ectodomains of the type I interferon receptor subunits ifnar1 and ifnar2 carrying a C-terminal decahistidine tag (ifnar1-H10 and ifnar2-H10, respectively) and their ligand IFNα2.[29] The proteins were expressed and purified as previously described.[30−32] Protein binding was monitored by imaging SPR using continuous flow injection analysis with a flow rate of 20 μL/min. All measurements were carried out in 50 mM Hepes, pH 7.4, and 150 mM NaCl containing 0.015% Tween 20. After conditioning the surface with 500 mM imidazole, the bis-NTA chelator heads were loaded by injection of 10 mM NiCl, followed by intensive rinsing. For characterizing the binding capacity of the array elements, 500 nM ifnar2-H10 was injected for 5 min. For studying ternary complex formation, ifnar1-H10 and ifnar2-H10 were sequentially injected at concentrations of 100 and 50 nM, respectively. For probing ligand binding, 2 μM of the

(24) Abelès, F. *Surf. Sci.* **1976**, *56*, 237−251.
(25) Poksinski, M.; Arwin, H. *Thin Solid Films* **2004**, *455−56*, 716−721.
(26) Westphal, P.; Bornmann, A. *Sens. Actuators, B* **2002**, *84*, 278−282.
(27) Raether, H. *Surface Plasmons on Smooth and Rough Surfaces and on Gratings*; Springer-Verlag: Berlin, Heidelberg, 1988.
(28) Ulman, A. *An Introduction to Ultrathin Organic Films from Langmuir−Blodgett to Self-Assembly*; Academic Press: San Diego, CA., 1991.
(29) Mogensen, K. E.; Lewerenz, M.; Reboul, J.; Lutfalla, G.; Uze, G. *J. Interferon Cytokine Res.* **1999**, *19*, 1069−1098.
(30) Lamken, P.; Lata, S.; Gavutis, M.; Piehler, J. *J. Mol. Biol.* **2004**, *341*, 303−318.
(31) Piehler, J.; Roisman, L. C.; Schreiber, G. *J. Biol. Chem.* **2000**, *275*, 40425−40433.
(32) Piehler, J.; Schreiber, G. *J. Mol. Biol.* **1999**, *289*, 57−67.

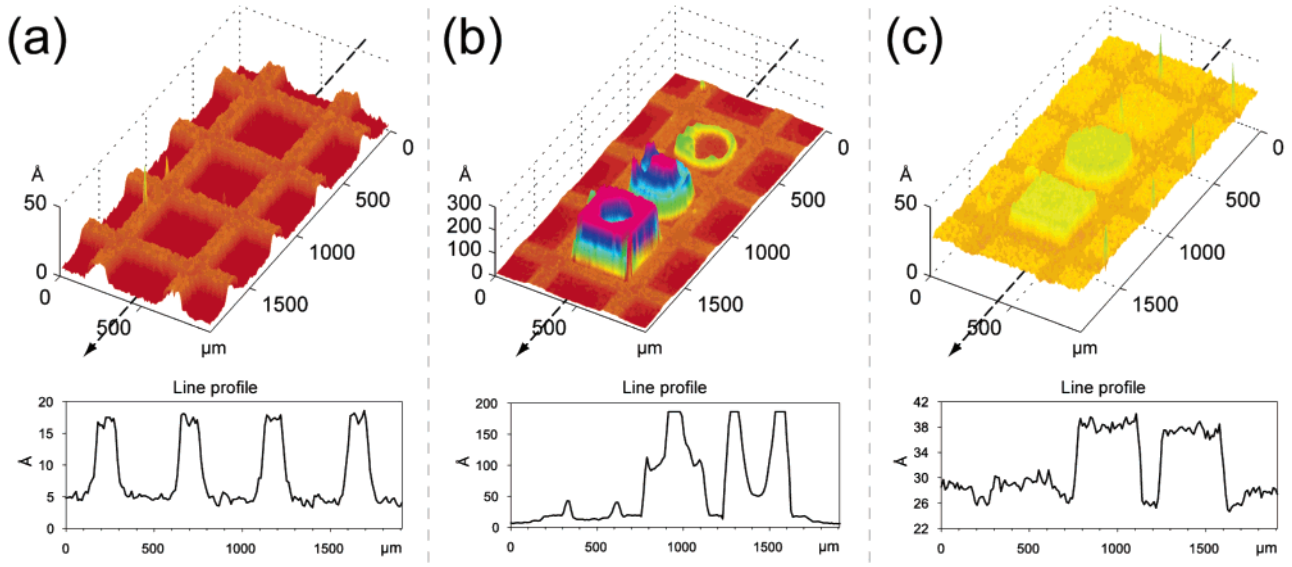

Figure 2. Thickness maps and line profiles of the chip at different stages in the process measured with imaging ellipsometry. Vertical scale represents layer thickness in Ångströms, and horizontal represents *x*/*y* dimension in micrometers. Line profiles have been obtained by averaging three adjacent lines, corresponding to a width of 34 μm. (a) The array biochip after printing the hydrophobic C_{20} barriers and (b) after dispensing three concentrations (0.02, 0.2, and 1 mM from top to bottom) of 50 mol % bis-NTA. Note that the instrument was unable to measure the full thickness range on this chip. (c) The biochip after back-filling with EG_3 and sonication in ethanol.

IFNα2 mutant M148A was used, which dissociates ~50 times faster from ifnar2-H10 (K_D ~150 nM) than wild-type IFNα2.[31] Still, its affinity toward ifnar1-H10 (K_D ~5 μM)[30,33] is more than 1 order of magnitude lower than toward ifnar2-H10.

Ligand dissociation curves from ifnar1-H10 and ifnar2-H10 coimmobilized on the surface were normalized to the total binding amplitude and fitted by a biexponential decay.

$$R(t) = R_{01}e^{-k_{d1}t} + R_{02}e^{-k_{d2}t} \quad (1)$$

The dissociation rate constants from binary and ternary complex, k_{d1} and k_{d2}, respectively, were fitted globally over all curves, whereas the corresponding binding amplitudes R_{01} and R_{02} were fitted locally for each curve ($R_{01} + R_{02} = 1$).

RESULTS AND DISCUSSION

Traditional piezo dispensing was employed to manufacture a density array of bis-NTA. To confine the dispensed sample volumes into defined geometries, a micropatterned grid of C_{20} was transferred to the gold surface using μCP. The squares defined by this hydrophobic grid were filled by applying several microdroplets of the ethanolic bis-NTA/EG_3 thiol solutions. The key challenge of this approach was to generate homogeneous SAMs within the array spots and, simultaneously, to avoid overflow and concomitant spillover between neighboring spots. This required thorough optimization of the dispensing procedure, including the concentration of the thiols as well as the volumes and the frequency of the applied microdroplets.

Concentration Effect. First, the role of the total thiol concentration in the dispensing solution on the homogeneity of the SAMs in the array elements was investigated. A mixture of 50 mol % bis-NTA in EG_3 was dispensed in three concentrations: 0.02, 0.2, and 1 mM. The high-percentage mixture was chosen to obtain a significant contrast in thickness between the printed C_{20} and the back-filled areas of EG_3 thiols. Imaging ellipsometry was used to characterize the array at different stages of the process: directly after μCP, after dispensing, and finally, after back-filling with EG_3 thiol and rinsing. The data are presented as thickness maps and line profiles (Figure 2).

Figure 2a shows the array after μCP of the C_{20} thiol. The resulting barrier displays an average thickness of 16.7 ± 0.8 Å. This is considerably less than the expected ~25 Å,[34] indicating incomplete C_{20} monolayer formation after printing. A higher C_{20} concentration in the ink during printing and a longer contact time may produce a more complete monolayer; however, the structural quality of the C_{20} monolayer is not critical in this particular case because the primary goal of the printing process is to produce hydrophobic barriers to confine the dispensed solutions and prevent spillover. It should be emphasized that a higher C_{20} concentration also may increase the risk of modifying the array elements (bare gold squares) by vapor deposition. A small amount of organic material is, in any case, deposited in the bare noncontact gold areas, as can be seen as an increase in thickness of 4.9 ± 1.0 Å after printing, indicating possible deposition of contaminants, most likely from airborne species or from residues of the PDMS stamp, an observation known from previous studies using μCP. These contaminants, however, are only weakly attached and can easily be removed upon exposure to the back-filling thiol solution.[23]

Figure 2b shows the array after dispensing of the three concentrations of 50% bis-NTA in the array elements. All the dispensed thiols are confined in their respective squares by the barriers; that is, no spillover is seen on the barriers or into the surrounding squares. The lowest concentration of 0.02 mM

(33) Gavutis, M.; Lata, S.; Lamken, P.; Muller, P.; Piehler, J. *Biophys. J.* **2005**, *88*, 4289−4302.

(34) Bain, C. D.; Troughton, E. B.; Tao, Y. T.; Evall, J.; Whitesides, G. M.; Nuzzo, R. G. *J. Am. Chem. Soc.* **1989**, *111*, 321−335.

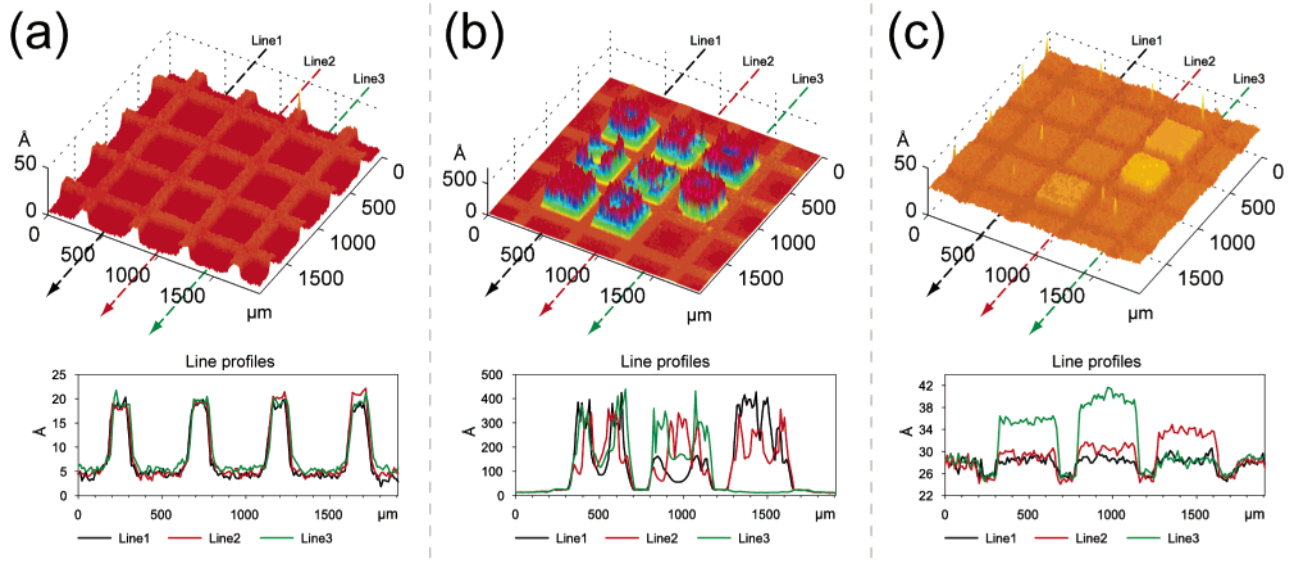

Figure 3. Thickness maps and line profiles of the biochip at different stages of the process characterized by imaging ellipsometry. Vertical scale represents layer thickness in Ångströms and horizontal represents *x*/*y* dimension in micrometers. Line profiles have been obtained by averaging three adjacent lines, corresponding to a width of 34 μm. (a) The chip after printing the hydrophobic C_{20} barriers and (b) after dispensing eight different molar ratios of bis-NTA (0, 1, 2, 5, 10, 20, 30, and 50 mol % from upper left to lower right) mixed with EG_3 at a total concentration of 1 mM. (c) The chip ready for use after back-filling in EG_3 and sonication in ethanol.

generates a classical coffee-ring pattern with a thickness of ~13 Å in the center of the ring and up to ~50 Å at the rim. The appearance of coffee rings and the underlying mechanism(s) have been thoroughly discussed by Deegan et al.[35] Thus, it appears to be enough material deposited at the rim, but not inside the ring, to give a complete monolayer of 50 mol % bis-NTA, which has been measured to equal 37 ± 0.8 Å for solution-prepared SAMs. For the 0.2 and 1 mM solutions, however, the amount of deposited materials is sufficient to obtain a full monolayer. The thinnest region is 50 Å and appears in the center of the 1 mM dispensed square, whereas the thickest regions are well above 180 Å, the maximum thickness reading for the instrumental setting used for this sample. The thickness of the untreated gold squares increases by another 2.9 ± 0.9 Å, possibly due to deposition of airborne contaminants. The hydrophobic C_{20} barriers, however, increase marginally in thickness.

Figure 2c shows the surface after the last step, which is after incubation in the EG_3 thiol back-filling solution and sonication in ethanol. The squares back-filled with EG_3 are now 28.5 ± 1.1 Å thick, a value in excellent agreement with the thickness obtained for a solution-prepared EG_3 SAM (28.6 ± 0.8 Å). Further on, the hydrophobic grid increases in thickness to 26.4 ± 1.0 Å, most likely because of partial incorporation of EG_3 molecules into the incomplete C_{20} monolayer.

A huge improvement can be seen in terms of homogeneity in all the dispensed squares due to removal of physisorbed thiols. For the two highest concentrations, the measured thicknesses are 38.2 ± 1.0 (0.2 mM) and 37.2 ± 1.1 Å (1 mM). These findings are again in very good agreement with the thickness of a densely packed monolayer generated from a 50% bis-NTA solution. However, for the 0.02 mM concentration, the thickness is only 29.3 ± 1.2 Å, which is very close to the thickness of the EG_3 SAM. These results indicate that a total thiol concentration of 0.02 mM is not sufficient to generate a complete SAM.

In conclusion, under the chosen conditions and for the thiols of interest, we decided to work with 1 mM solutions, although 0.2 mM seems to be enough to produce a full monolayer of the 50% bis-NTA-mixture. The high concentration (1 mM) is usually not desired to avoid overloading and spillover of the thiol material. It may also restrict the conformational freedom of the molecules during the SAM formation. As a consequence, it is likely that we compromised the structural perfection of this fairly complex SAM to achieve the desired functional properties of the array. However, it should not be forgotten that in the case of defects in the dispensed SAM, the EG_3 molecules from the subsequent back-filling solution are still available for improving the structural quality of the monolayer and, thereby, the presentation of the bis-NTA groups.

Dispensing the bis-NTA Array. A chelator array was generated by dispensing different molar mixtures of bis-NTA. The total thiol concentration for dispensing was chosen as 1 mM to ensure homogeneous filling of the array elements. Mixtures of 0, 1, 2, 5, 10, 20, 30, and 50 mol % bis-NTA were dispensed on the chip. The results are shown in Figure 3 at the same stages of the process as described above. Once again, it can be seen that the printing produces barriers of C_{20}, although incomplete, with a thickness of 18.6 ± 1.2 Å (Figure 3a). The untreated gold squares are 5.0 ± 1.0 Å thick, in good agreement with previous samples.

Figure 3b shows an array generated by successively dispensing eight bis-NTA mixtures. All eight areas are sufficiently filled with thiols with thicknesses ranging from roughly 60 to 400 Å. These excessive multilayers are efficiently removed after incubation in the EG_3 back-filling solution (Figure 3c). Note that the ellipsometric image shows a gradually increasing SAM thickness for an increasing mol % of bis-NTA, ranging from 28.2 ± 1.3 Å (0%) to 39.4 ± 1.3 Å (50%). Interestingly, we found only a negligible

(35) Deegan, R. D.; Bakajin, O.; Dupont, T. F.; Huber, G.; Nagel, S. R.; Witten, T. A. *Nature* **1997**, *389*, 827−829.

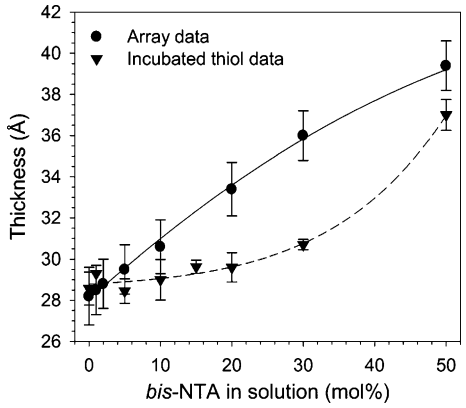

Figure 4. Comparison of thicknesses of the SAMs obtained by dispensing mixtures of bis-NTA on an array and by solution incubation. The lines have been added as a guide for the eye.

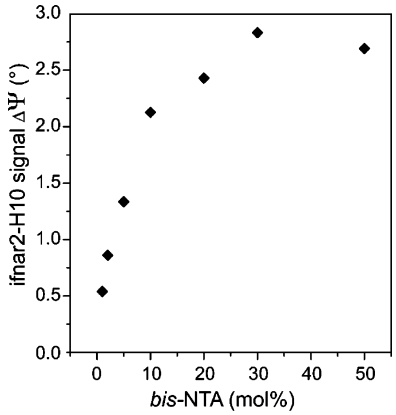

Figure 5. Immobilization levels (ΔΨ) of 500 nM ifnar2-H10 (5-min injection) on the chip as a function of the bis-NTA mixture dispensed in the array elements, measured with imaging SPR.

difference in the thickness of dispensed EG_3 (28.2 ± 1.3 Å) and the one generated by back-filling with EG_3 (28.6 ± 1.3 Å). In addition, a comparison between the 50 mol % bis-NTA dispensed on this array and the previous one displays only a small variation in thickness, 39.4 ± 1.3 Å, as compared to 37.2 ± 1.1 Å (Figure 2); however, there seems to be an extra adlayer of thiols left on the latter chip for this ratio, because a "hump" can be seen on the line profile over this square (∼2−3 Å thicker in the middle) but not on any of the other squares, which appear flat. We believe that additional sonication treatment or optimized ambient conditions, for example, lowering of the pH with HCl or TFA or conditioning the surface with EDTA and Ni^{2+} ions, will improve the homogeneity of the dispensed 50 mol % bis-NTA SAMs.

The thicknesses, after back-filling and sonication, for each of the dispensed concentrations are plotted in Figure 4. Also plotted in this figure, for comparison, are thicknesses measured with null-ellipsometry for monolayers prepared under equilibrium-like conditions, that is, for gold surfaces immersed into solutions of bis-NTA and EG_3 in ethanol at a total concentration of 20 μM for 24 h. The thicknesses of the dispensed layers agree very well with those prepared by solution deposition for low molar ratios of bis-NTA. However, the thicknesses start to deviate above 10%, reaching a maximum deviation at ∼30%. The formation of self-assembled monolayers is, in itself, a complicated process which involves different intermediate structures and island growth on the surface.[36,37] The presence of the rather bulky bis-NTA group certainly affects this process because of steric effects and complex intermolecular interactions. Additionally, the short time available for in-plane organization on the surface together with the relatively high concentration create conditions that are far from equilibrium. Thus, the observed differences in thickness between the spotted and solution-prepared SAMs for the molar ratios 10−50% are not surprising. It seems that the probability of sticking to the surface is higher for bis-NTA when the concentration of the solution increases (during evaporation), leading to a SAM with preferentially adsorbed bis-NTA molecules. Nevertheless, for mixtures below 10% bis-NTA, this effect is not very pronounced, at least not with ellipsometry. A detailed investigation with IR microscopy will be undertaken to address the structural characteristics of the dispensed SAMs (to be published elsewhere). Thus, the comparison in Figure 4 suggests that the mechanism or kinetics of formation are different for the piezo-dispensed and solution-deposited SAMs.

Functional Properties. Dispensing the bis-NTA thiol at different molar ratios yielded a surface concentration array of the high-affinity chelator headgroup. The array offers the possibility to simultaneously immobilize histidine-tagged proteins at different surface compositions (surface densities). Figure 5 shows binding levels (ΔΨ) after 500 nM ifnar2-H10 has been injected over the surface for 5 min. The immobilization of ifnar2-H10 increases rapidly up to 10 mol %, above which it starts to level off and saturate at roughly 30 mol %, most likely because of steric constraints.

Such an array was employed to study ligand-induced cross-linking of the type I interferon receptor (Figure 6a). The ectodomains of the receptor subunits ifnar1 and ifnar2 fused to a C-terminal decahistidine-tag (ifnar1-H10 and ifnar2-H10, respectively) are specifically tethered to the bis-NTA, as previously shown.[19] During injection of the high-affinity subunit ifnar2-H10, signals between 0.1° and 0.7° in the ellipsometric parameter Ψ are obtained, depending on the bis-NTA surface concentration, while no significant binding is observed on the 0% reference spot (Figure 6b, the injection denoted by I). Moreover, the protein level remains stable on the surface at all surface concentrations employed. For the ligand IFNα2 M148A, fully specific, reversible binding is observed (Figure 6b, injection II). The relative ligand binding capacity of ifnar2-H10 and the ligand dissociation kinetics are basically independent of the absolute ifnar2-H10 surface concentrations (Figure 6c), confirming full functionality of ifnar2-H10 on the surface and a 1:1 interaction with IFNα2. After dissociation of the ligand, a 1:1 molar ratio of ifnar1-H10 (50 kDa) relative to ifnar2-H10 (25 kDa) is loaded onto the surface (Figure 6b, injection III), and IFNα2 M148A is injected again (Figure 6b, injection IV). Ifnar1-H10 alone hardly interacts with IFNα2 M148A under these conditions (K_D ∼5 μM, k_d ∼ 1 s^{-1}). Nonetheless, a variation in dissociation kinetics is observed, which decreases with increasing receptor surface concentration (Figure 6d). This effect is ascribed to a ternary complex formation governed by simultaneous interaction with ifnar2-H10 and ifnar1-H10, which has been shown to be very efficient on laterally fluid solid-supported membranes.[30] The dissociation curves were fitted to a global

(36) Schreiber, F. *Prog. Surf. Sci.* **2000**, *65*, 151−256.
(37) Schwartz, D. K. *Annu. Rev. Phys. Chem.* **2001**, *52*, 107−137.

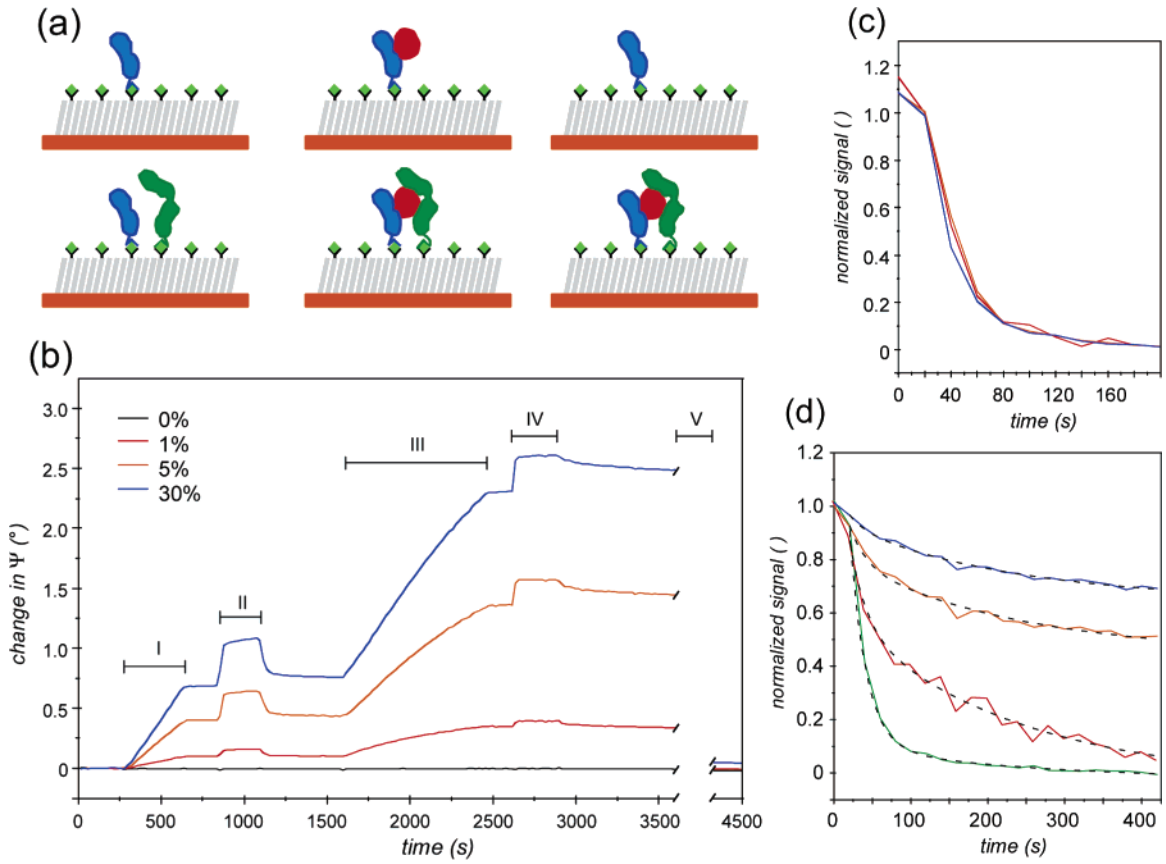

Figure 6. Ternary protein complex studied by imaging SPR with a spotted array of bis-NTA at various surface concentrations. The sensorgrams have been corrected for the background signal (BSA-covered C_{20} SAM). (a) Schematic illustration of the interaction assay: after immobilization of ifnar2-H10 (blue), the ligand (red) binds transiently due to its low affinity (top panel). After subsequent immobilization of ifnar1-H10 (green), a ternary complex by cross-linking of ifnar2-H10 and ifnar1-H10 can be formed. (b) Sensorgrams for 0, 1, 5, and 30 mol % bis-NTA in comparison. Note that sensorgrams for the intermediate- and high-concentration mixtures have been omitted to give a clearer overview of the results. I, injection of 50 nM ifnar2-H10; II, injection of 2 μM IFNα2-M148A; III, injection of 100 nM ifnar1-H10; IV, injection of 2 μM IFNα2-M148A; and V, injection of 1 M imidazole. (c) Overlay of the ligand dissociation curves of injection II (signals normalized to the equilibrium signals). (d) Overlay of ligand dissociation curves of injection IV (signals normalized to the equilibrium signals) and fitted global biexponential decay curves (dotted lines) (see text). The dissociation from ifnar2-H10 alone (injection II) is shown for comparison (green line) with fitted monoexponential decay curve (dotted line).

biexponential decay function (eq 1), yielding the two dissociation rate constants $k_{d1} = 0.048\ s^{-1}$ and $k_{d2} = 8 \times 10^{-4}\ s^{-1}$. The k_{d1} is in good agreement with the dissociation rate constant of the binary complex, $0.045\ s^{-1}$ (injection II, Figure 6b–d), whereas k_{d2} represents the dissociation rate constant from the ternary complex. This result is in line with binding studies on solid-supported membranes, where ~100-times slower ligand dissociation from the ternary complex has been observed, as compared to the binary complex.[30] The preexponential amplitude R_{02}, representing the fraction of ligand in the ternary complex, increases with surface concentration and is observed as to equal 0.57 at 1 mol % bis-NTA, 0.79 at 5 mol %, and 0.90 at 30 mol %. Thus, the ternary complex formation requires immobilization of ifnar1-H10 and ifnar2-H10 in close proximity, which is more probable at high surface concentrations. In the case of a substantial affinity between the receptor subunits without the ligand, ternary complex formation should not be dependent on the surface concentration. Therefore, simultaneous monitoring of protein interactions at various surface concentrations provides a powerful means to dissect protein–protein interactions. Furthermore, the regeneration of the chip is readily achieved with an injection of 1 M imidazole (Figure 6b, event V), enabling multiple use of the same chip.

CONCLUSIONS

This contribution describes the fabrication of a versatile microarray platform capable of capturing His-tagged proteins in an oriented and functional manner. Hydrophobic barriers generated by μCP were introduced on the gold surface to facilitate piezo-dispensing of bis-NTA-terminated thiols and to prevent overflow and spillover between neighboring spots. The generated array was relatively small, 3 × 3, but it can easily be extended by employing state-of-the-art equipment for precise, computer-controlled dispensing and repeatable μCP. The various stages in the fabrication process were thoroughly characterized with imaging ellipsometry, and functional tests were undertaken with imaging SPR.

Consistently increasing levels of stable and functionally intact proteins (receptors) were obtained with increasing surface concentration of bis-NTA, and the application of the generated array for studies of cooperative interactions, leading to the formation of a ternary protein complex (receptor–ligand–receptor) was successfully demonstrated. Because the His-tagged proteins are

readily removed from the surface upon exposure to a pulse of imidazole, versatile and automated assay formats with different protein concentrations and injection sequences can be carried out on the same biochip. Thus, the bis-NTA density array provides a means for studying multiprotein complex formation as well as for optimizing the assembly process of multiprotein complexes on solid supports. Moreover, spotting arrays of functional SAMs can further be envisioned as a powerful tool for multiplexing protein immobilization and, hence, generating protein biochips for functional proteomics.

ACKNOWLEDGMENT

This research was supported by the Wallenberg Consortium North (WCN), the Swedish Research Council (VR), and the Swedish Foundation for Strategic Research (SSF) through the Biomimetic Materials Science program. This work was also supported by the German Research Council (DFG, Pi-405/1, Pi-405/2, and Ta-157/6) and by the German Ministry of Education and Research (BMBF, 0312005A). R.V. acknowledges support from the Lithuanian State Science and Studies Foundation and the Swedish Institute through the Visby program.

Received for review January 5, 2006. Accepted March 28, 2006.

AC060024+